Journal of Sound and Vibration (1997) **208**(1), 33–45

NON-LINEAR DYNAMIC IDENTIFICATION: AN APPLICATION TO PRESTRESSED CABLE STRUCTURES

G. E. B. Tan and S. Pellegrino

Department of Engineering, University of Cambridge, Trumpington Street, Cambridge CB2 1PZ, England

(*Received* 14 *March* 1996, *and in final form* 21 *May* 1997)

The paper presents a robust implementation of the restoring force method, which is applied to the dynamic identification of two simple prestressed cable structures. The system parameters identified from two different types of dynamic experiments are found to be generally in good agreement with the parameters calculated from direct static measurements. Hence, general conclusions are reached on optimal identification strategies for lightweight non-linear structures.

1. INTRODUCTION

This paper is concerned with the experimental identification of geometrically non-linear structures. The method used is generally known as "restoring force surface method" [1] or "force state mapping" [2] which has a direct physical meaning, is easy to implement, and can be used in a variety of different situations. Previous applications have been focussed on systems whose non-linearities are not known *a priori* [1, 3–5]. In this paper, the restoring force surface method is applied to a class of structures whose geometrically non-linear properties are known, and hence the coefficients of the non-linear system of equations of motions can be calculated from direct measurements. For such systems the identification technique can be validated by comparing the directly measured system parameters to the system parameters estimated by considering restoring force functions.

The first structure that has been investigated consists of a small rigid element attached to the middle of a prestressed, straight steel cable, which was excited in a transverse direction. This structure can be modelled as a single-degree-of-freedom (SDOF) system. For small displacements, the cable behaves as a linear spring whose stiffness is proportional to the level of prestress. As the excitation amplitude increases a cubic non-linearity appears, of magnitude proportional to the axial stiffness of the cable. The second structure that was investigated consists of two parallel, prestressed cables connected by a slender, rigid element whose out-of-plane motion can be modelled in terms of two degrees of freedom. The geometrically non-linear behaviour of these two structures is typical of cable structures in general, see references [6, 7].

For each of these structures, the correct coefficients of the equations of motion can be obtained from direct static measurements, and can thus be compared to the coefficients estimated by means of the restoring force method, without making use of any information on the special features of the particular system. This comparison is carried out by

0022–460X/97/460033 + 13 $25.00/0/sv971130

estimating best-fit system parameters for a gradually increasing number of non-linear terms in the equations of motion. For each set of parameters, the response of the system is simulated in order to estimate the corresponding error with the experimental data. It is found that, in general, the inclusion of terms of the correct order leads to significant error reductions, but that a residual error exists due to noise in the experimental data.

The layout of this paper is as follows. The next section gives a brief description of the theory behind the restoring force method, followed by an explanation of the way in which the set of system parameters can be identified from experimental data. In section 3 the theoretical models are derived for the two cable systems that are investigated, from which the key experimental parameters are selected. In section 4 the identification experiments and the analysis of the experimental data leading to the identification of system parameters are presented. Section 5 contains discussion of the results obtained from this study and concludes the paper.

2. THE RESTORING FORCE METHOD

The equation of motion of a SDOF non-linear system can be written, by an obvious extension of the standard linear case, in the form

$$m\ddot{y} + \sum_j c_j \dot{y}^j + \sum_j k_j y^j = F, \tag{1}$$

where m is the mass, y, $\dot{y}$ and $\ddot{y}$ its displacement, velocity and acceleration, and F is the external force. The coefficients c_1, k_1 are respectively the standard viscous damping and stiffness coefficients, while c_2, k_2, etc., are the coefficients of higher order damping and stiffness terms. Equation (1) is valid on the assumption that there is neither coupling between velocity and displacement, nor between stiffness terms of different order. However, the formulation presented in this paper could be easily modified to include such effects, if required.

With equivalent assumptions, equation (1) may be extended to multi-degree-of-freedom (MDOF) systems where, upon assuming coupling between displacements only, the ith equation of motion may be written as

$$m_i \ddot{y}_i + \sum_j c_{ij} \dot{y}_i^j + \sum_j k_{ij} y_i^j + \sum_{j \neq i,l,m} k_{ijlm} y_i^l y_j^m = F_i. \tag{2}$$

Other terms, such as displacement–velocity coupling could be included and the final form of the equation of motion may include all possible terms of a certain type, or a reduced number of terms that have been selected according to some special features of the particular problem that is analysed.

If the mass associated with degree-of-freedom i is known, then the corresponding restoring force is defined as follows, from equation (2):

$$f_i = F_i - m_i \ddot{y}_i = \sum_j c_{ij} \dot{y}_i^j + \sum_j k_{ij} y_i^j + \sum_{j \neq i,l,m} k_{ijlm} y_i^l y_j^m. \tag{3}$$

According to equation (3), f_i is a function of y_i and $\dot{y}_i$, and also of all the other displacements DOFs. If, however, f_i is found to be insensitive to the other DOFs and hence it is a function of y_i and $\dot{y}_i$ only, then it can be plotted over the phase plane $(y_i, \dot{y}_i)$ and this plot is known as a force state map. Obviously, for a linear SDOF system the force

state map is a plane whose slopes with respect to displacement and velocity are respectively the linear stiffness and viscous damping coefficients. System non-linearities will distort the force state map. Once the number of parameters to be considered has been decided, their values can be estimated by conducting suitable experiments and by imposing a least squares fit between the measured force state map and its analytical expression.

An equivalent procedure can be followed when the mass m_i is not known and the coupling between different DOFs does not allow the plotting described above. In such cases, all unknown system parameters, including m_i, are estimated by a least squares fit between the measured excitation force F_i and its predicted value. It is this more general case that is considered in the next section.

2.1. IMPLEMENTATION

The idea is to take a series of measurements of displacement, velocity and acceleration of each DOF, together with the applied force, at several time steps, but measuring all of these quantities simultaneously is usually impractical. Hence, the normal practice is to measure the force and a limited number of states, and to compute the corresponding values of the remaining states. The approach taken in this work is to measure acceleration at regular time steps, and to obtain velocity and displacement by integration. Both time domain and frequency domain integration have been considered [8]. Time domain integration requires the use of high pass filters to remove low frequency noise which would otherwise be amplified at each integration step. For single frequency excitation, this technique has been found to be less reliable than the alternative technique. Hence, the integrated signals are obtained from the Fourier transform of $\ddot{y}$,

$$\dot{y}(\omega) = \ddot{y}(\omega)/\mathrm{j}\omega, \qquad y(\omega) = -\ddot{y}(\omega)/\omega^2,$$

where $\omega = 2\pi \times$ frequency, and $\mathrm{j} = \sqrt{-1}$. These relationships are used at all frequencies except $\omega = 0$, where it is assumed that $y(0) = \dot{y}(0) = 0$.

Once the states of the system and the corresponding force inputs are known, the identification process can begin. Consider, for example, a SDOF system that, in addition to the standard linear terms, is to be modelled by including quadratic and cubic stiffness terms. Thus, equation (1) gives

$$m\ddot{y} + c_1\,\dot{y} + k_1\,y + k_2\,y^2 + k_3\,y^3 = F. \tag{4}$$

Assume that s data samples have been taken, where the nth sample includes $\ddot{y}_n$, $\dot{y}_n$, y_n, and F_n. Substituting these values into equation (4) yields

$$m\ddot{y}_n + c_1\,\dot{y}_n + k_1\,y_n + k_2\,y_n^2 + k_3\,y_n^3 = F_n, \tag{5}$$

which is a linear equation in the five unknowns m, c_1, k_1, k_2, k_3. Considering all samples one obtains the following system of linear equations:

$$\begin{bmatrix} \ddot{y}_1 & \dot{y}_1 & y_1 & y_1^2 & y_1^3 \\ \ddot{y}_2 & \dot{y}_2 & y_2 & y_2^2 & y_2^3 \\ \cdot\cdot & \cdot\cdot & \cdot\cdot & \cdot\cdot & \cdot\cdot \\ \cdot\cdot & \cdot\cdot & \cdot\cdot & \cdot\cdot & \cdot\cdot \\ \cdot\cdot & \cdot\cdot & \cdot\cdot & \cdot\cdot & \cdot\cdot \\ \ddot{y}_{s-1} & \dot{y}_{s-1} & y_{s-1} & y_{s-1}^2 & y_{s-1}^3 \\ \ddot{y}_s & \dot{y}_s & y_s & y_s^2 & y_s^3 \end{bmatrix} \begin{bmatrix} m \\ c_1 \\ k_1 \\ k_2 \\ k_3 \end{bmatrix} = \begin{bmatrix} F_1 \\ F_2 \\ \cdot\cdot \\ \cdot\cdot \\ F_{s-1} \\ F_s \end{bmatrix}. \tag{6}$$

The matrix form of equation (6) is

$$\mathbf{A}\mathbf{x} = \mathbf{b}, \tag{7}$$

where $\mathbf{x}$ is a (5×1) column matrix containing the system parameters to be determined, $\mathbf{A}$ is the $(s \times 5)$ matrix containing the states of the system (and their powers), and $\mathbf{b}$ is a column matrix $(s \times 1)$ containing the measured force.

If the mass m is known, $\mathbf{b}$ is replaced by the restoring forces and the first column of $\mathbf{A}$ is removed.

Equation (7) is a largely over-determined system of equations that can be solved by least squares in order to minimize the errors induced by signal noise, numerical integration, etc. To guard against possible ill-conditioning (e.g., caused by the excitation amplitude being too small for a particular type of non-linearity to show up clearly), one computes the singular value decomposition of $\mathbf{A}$ [9].

Let σ_{ii} be the ith singular value, and $\mathbf{u}_i$, $\mathbf{v}_i$ the corresponding left and right singular vectors. Let r be the number of non-zero singular values. The threshold below which a singular value is deemed to be zero is set on the basis of machine precision as well as the level of noise present in the data [9].

The least squares solution of equation (7) is given by

$$\hat{\mathbf{x}} = \sum_{i=1}^{r} \frac{\mathbf{u}_i \cdot \mathbf{b}}{\sigma_{ii}} v_i. \tag{8}$$

The accuracy of the estimated parameters is assessed by means of a normalized root mean square error, which is defined as

$$e = \| \mathbf{A}\hat{\mathbf{x}} - \mathbf{b} \| / \| \mathbf{b} \| = \sqrt{\sum_{i=r+1}^{s} (\mathbf{u}_i \cdot \mathbf{b})^2} \Big/ \| \mathbf{b} \|. \tag{9}$$

The magnitude of e also acts as an indicator of the number of system parameters required to fit the experimental data. The number of terms in the model is increased until e falls below a preset threshold.

3. EXPERIMENT DESIGN

The first experiment is an investigation of the behaviour of a simple cable structure consisting of a small rigid mass attached to the mid-span of a single cable stretched between two fixed points, as shown in Figure 1. When displaced in a lateral direction, this system exhibits geometric non-linearity. Consider a cable of length $2L$ and axial stiffness EA,

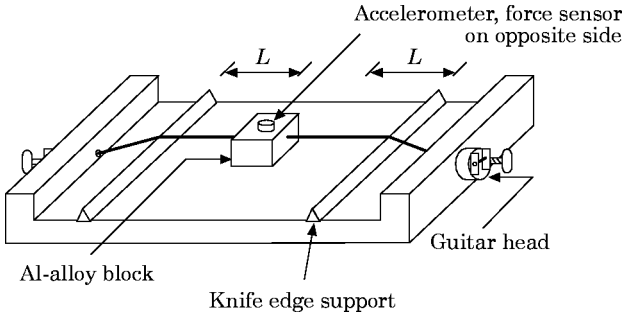

Figure 1. Set-up of first experiment.

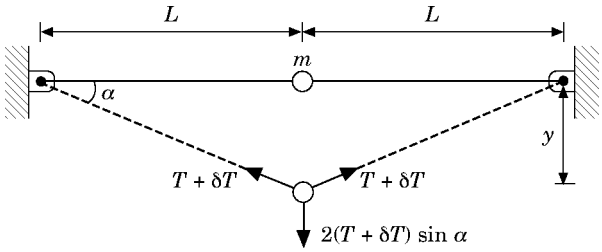

Figure 2. SDOF cable structure subject to a small displacement y, schematic layout.

subject to an initial tension T. If a small lateral displacement is imposed to the mid-point of this cable (see Figure 2) its tension increases by

$$\delta T = EA(\delta L/L) \approx EA(y^2/2L^2). \tag{10}$$

Hence, the static force required to impose a lateral displacement y is

$$2(T + \delta T)\sin\alpha \approx 2(T + EAy^2/2L^2)y/L = (2T/L)y + (EA/L^3)y^3 \tag{11}$$

According to equation (11) the lateral stiffness of this cable is the sum of a linear term and a cubic term, and hence the equation of motion in the transverse direction can be written as

$$m\ddot{y} + c_1\dot{y} + k_1 y + k_3 y^3 = F, \tag{12}$$

where $k_1 = 2T/L$ and $k_3 = EA/L^3$.

Numerical simulations based on equation (12) have been used to design an experiment where a sufficient amount of non-linear behaviour is produced with a maximum displacement amplitude of ± 5 mm, due to physical limitations of the available shaker. Thus, a stainless steel cable with diameter of 0·8 mm was chosen ($EA = 30$ kN) and it was stretched over two knife-edge supports to ensure consistent end conditions. Both ends of the cable were coiled around guitar machine heads, to allow a fine adjustment of cable tension. The cable tension, measured with a tension transducer [10] before clamping the block to the cable, was 45·3 N. A rigid block consisting of two Al-alloy parts was clamped on the cable, thus forming a cube with side length of 30 mm. The distance between a support and the side of the cube was $L = 0{\cdot}13$ m. A PCB miniature accelerometer and a force sensor were mounted on either side of this block whose mass, including transducers, was 0·104 kg. This set-up is shown in Figure 1.

The coefficients m, k_1, and k_3 that appear in equation (12) have been estimated from the physical dimensions and properties given above; see Table 1.

The second experiment is an investigation of the behaviour of a flat grid structure consisting of an Al-alloy "rigid" beam clamped to two parallel cables like those used in the first experiment, mounted at a distance of $2W$. The vibration of the beam in the

TABLE 1

System parameters for SDOF system

Parameter	Direct measurement	Shaker test	Free decay test
m (kg)	0·104	0·105	—
c (Ns/m)	—	0·44	0·28
k_1 (N/m)	$6{\cdot}98 \times 10^2$	$7{\cdot}01 \times 10^2$	$6{\cdot}97 \times 10^2$
k_3 (N/m^3)	$1{\cdot}33 \times 10^7$	$1{\cdot}37 \times 10^7$	$1{\cdot}16 \times 10^7$

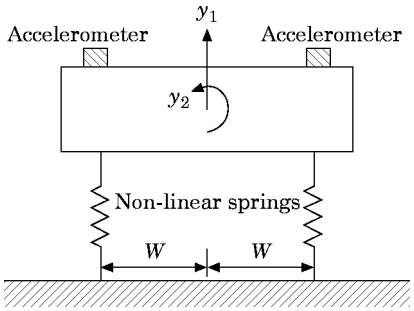

Figure 3. Idealized 2 DOF system.

direction perpendicular to the plane of the cables can be modelled in terms of a 2 DOF system consisting of a rigid lamina, representing the beam, supported by two non-linear springs, representing the cables, as shown in Figure 3. The stiffness relation for each spring is analogous to equation (11) and hence the static force required to impose a pure translation y_1 is

$$2[(2T/L)y_1 + (EA/L^3)y_1^3]. \tag{13}$$

Therefore, the translational equation of motion is

$$m_1\,\ddot{y}_1 + c_{11}\,\dot{y}_1 + k_{11}\,y_1 + k_{13}\,y_1^3 = F_1. \tag{14}$$

To find the second equation of motion a static rotation y_2 is imposed, after imposing a translation y_1. Since the right side and left side springs have stretched by $y_1 + Wy_2$ and $y_1 - Wy_2$ respectively, the forces applied to the lamina by these springs are respectively

$$(2T/L)\,(y_1 + Wy_2) + (EA/L^3)\,(y_1 + Wy_2)^3, \tag{15}$$

$$(2T/L)\,(y_1 - Wy_2) + (EA/L^3)\,(y_1 - Wy_2)^3. \tag{16}$$

Upon taking moments about the centre of the lamina, the couple required for static equilibrium is found to be

$$(4TW^2/L)y_2 + (3EAW^2/L^3)y_1^2y_2 + (EAW^4/L^3)y_2^3 = F_2 \tag{17}$$

and hence the rotational equation of motion may be written in the form

$$m_2\,\ddot{y}_2 + c_{21}\,\dot{y}_2 + k_{21}\,y_2 + k_{23}\,y_2^3 + k_{1221}\,y_1^2y_2 = F_2, \tag{18}$$

where m_2 is the moment of inertia of the lamina, F_2 is the externally applied torque, $k_{21} = 4TW^2/L$, $k_{23} = 2EAW^4/L^3$, and $k_{1221} = 6EAW^2/L^3$.

As in the first experiment, numerical simulations have been carried out to determine appropriate system parameters for which reasonable amounts of non-linear behaviour would be observed. For the same type and length of cable as in the first experiment, the dimensions of the block were chosen to be $0{\cdot}12 \times 0{\cdot}02 \times 0{\cdot}018\ \mathrm{m}^3$, the prestress was set at 44·2 N, and the distance $2W$ between the two cables was 0·1 m. The corresponding theoretical estimates of the coefficients of equations (14) and (18), apart from the damping coefficients, are given in Table 2.

Two accelerometers were used to record the response. These were placed symmetrically about the centre of mass, at each end of the Al-alloy block. The translational data was obtained by averaging the two responses, and the rotational data from their difference.

TABLE 2

System parameters for 2 DOF system

Parameter	Direct measurement	Shaker test	Free decay test
m_1 (kg)	0·202	0·21	—
c_{11} (Ns/m)	—	0·54	0·25
k_{11} (N/m)	$1{\cdot}31 \times 10^3$	$1{\cdot}34 \times 10^3$	$1{\cdot}30 \times 10^3$
k_{13} (N/m^3)	$2{\cdot}18 \times 10^7$	$2{\cdot}12 \times 10^7$	$1{\cdot}91 \times 10^7$
m_2 (kgm^2)	$3{\cdot}18 \times 10^{-4}$	$3{\cdot}34 \times 10^{-4}$	—
c_{21} (Nms/rad)	—	$1{\cdot}25 \times 10^{-2}$	$8{\cdot}81 \times 10^{-4}$
k_{21} (Nm/rad)	3·15	3·22	3·04
k_{23} (Nm/rad^3)	$1{\cdot}31 \times 10^2$	$1{\cdot}43 \times 10^2$	$1{\cdot}20 \times 10^2$
k_{1221} (N/m)	$3{\cdot}27 \times 10^5$	$2{\cdot}87 \times 10^5$	$3{\cdot}60 \times 10^2$

4. IDENTIFICATION TESTS

The response of each cable system was measured for two different types of excitation, a constant frequency sinusoid of linearly varying amplitude—applied through a pair of coil-type shakers—and a static imposed displacement. A personal computer fitted with a National Instruments digital board was used to output the excitation signals, which were amplified by using PA100 power amplifiers, and to take force and acceleration measurements. The board operates in a sequential mode, but the time delay between consecutive channels (5 μs) is sufficiently small that the associated phase error is negligibly small. Noise effects were removed by applying rectangular windows with a bandwidth of 1 Hz at harmonics of the forcing frequency.

4.1. SDOF CABLE STRUCTURE

The first test was conducted with an excitation signal consisting of a ramped sine wave at 8·5 Hz over a total period of 10·24 seconds, with data samples taken at 400 Hz over the full duration of the test. The force and acceleration response measurements are shown in Figure 4, while Figure 5 shows the restoring force map where the mass of the system

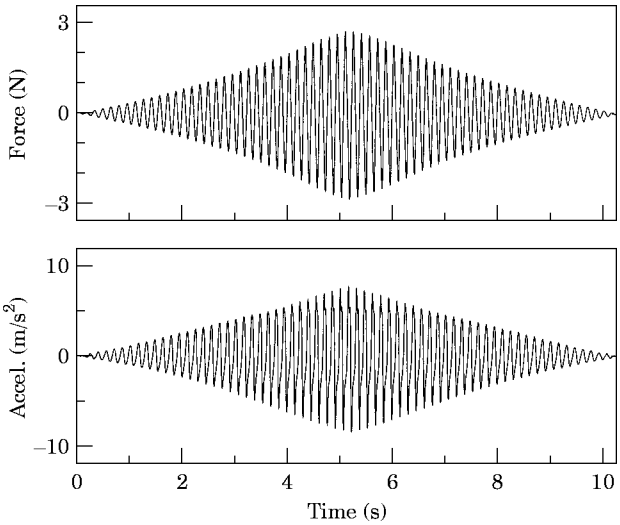

Figure 4. Force and acceleration measurements.

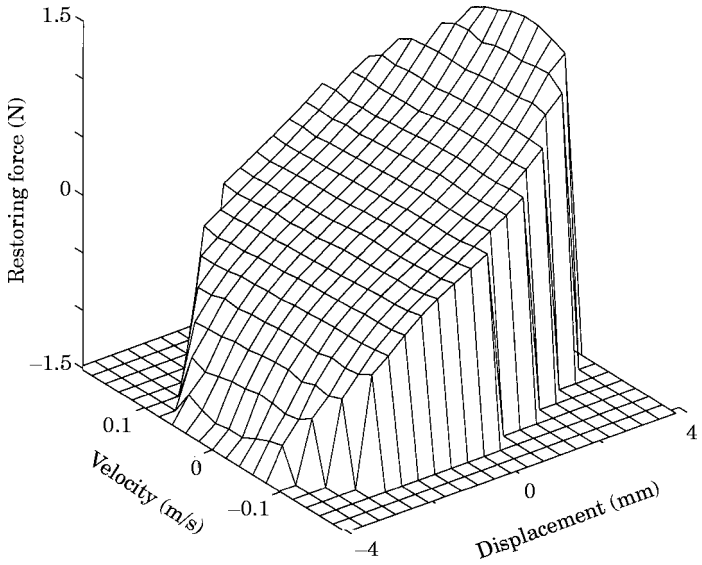

Figure 5. Force state map of SDOF system.

has the value obtained by direct measurements. To show the cubic stiffness effects more clearly, 70% of the linear stiffness has been removed before plotting the data.

The identification method described in section 2 has been applied to the experimental data, with a gradual increase in the number of system parameters included in the model. The number of stiffness terms has been varied from 1, linear stiffness, to 10: i.e., including terms up to $k_{10}\,y^{10}$. Similarly, the number of damping terms has been increased from 0, no damping, to 10. Figure 6 shows the variation in the corresponding error e. Increasing the stiffness terms from one to two does not make much difference, because k_2 has no physical basis, but the inclusion of a third term leads to a significant reduction in error. The inclusion of further terms has practically no effect. The variation of e with the number of damping terms shows a steep drop when the first term is included, but hardly any subsequent improvement. Once the physically significant third order stiffness term and first order damping term have been included in the model, e becomes practically constant; the residual error can be attributed to signal noise. Hence, the parameters that have been

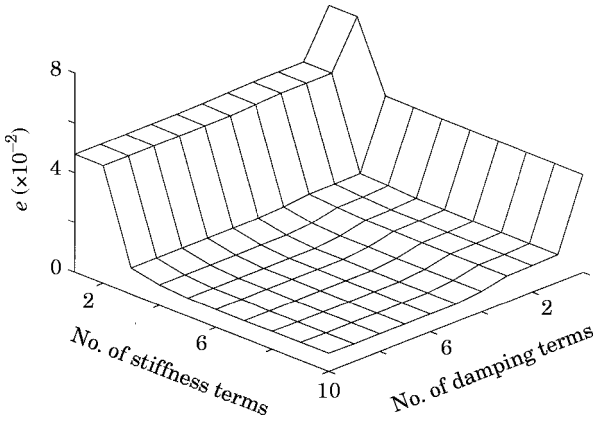

Figure 6. Error plot for SDOF cable system (shaker test data).

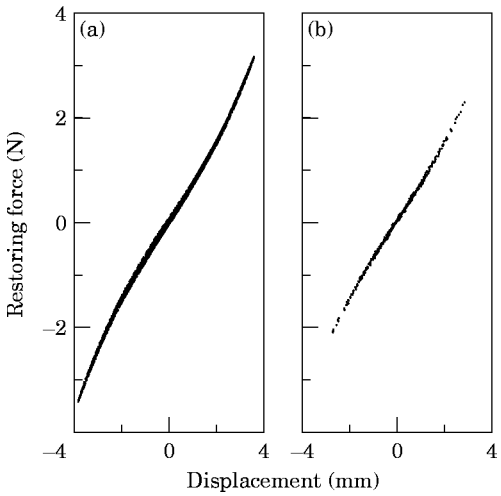

Figure 7. Restoring force plots for SDOF system: (a) forced vibration; (b) free decay.

estimated are m, c_1, k_1 and k_3: their values are given in Table 1. Note that both the estimated mass and stiffness parameters are very close to the expected values. Also note that the damping coefficient corresponds to a damping ratio of $\zeta = 2{\cdot}6\%$ but, at this stage, there is no reference value to compare it with.

The above results have been obtained by considering the full set of 4096 data points. In order to investigate the sensitivity of the estimated parameters to different data sampling strategies, the parameter estimation has been repeated using data samples taken during the following time periods: (0–5·12 s), (1·28–5·12 s) and (2·56–5·12 s). It has been found that the coefficients of the linear terms are practically unaffected, and the non-linear terms are also unaffected if the sampled data covers a sufficiently large range of the restoring force map. Thus, there are practically no changes if the data spans the range (0–5·12 s), and the worst result is an increase of k_3 by 15% for the range (2·56–5·12 s).

The second test was conducted by applying a vertical static displacement to the mass, and measuring the free decay response obtained after releasing the mass. Because $F = 0$ in this test, m must be known in order to estimate the system parameters. The parameters estimated from this test are shown in the last column of Table 1. Again the stiffness parameters estimated are very close to the values obtained from direct measurement.

Figure 7 shows side views of the force state maps obtained from the two tests. These plots show clearly that the cubic stiffness effects are more marked in the first test, and hence the k_3 coefficient that is estimated from the shaker test would be expected to be more accurate. Indeed, this is what is found in Table 1.

Next, consider the damping coefficient. The value of c_1 estimated from the first test is 0·44 ($\zeta = 2{\cdot}6\%$) while the value estimated from the second test is 0·28 ($\zeta = 1{\cdot}6\%$). This discrepancy is due to the added damping associated with the shaker, in the first test, which has been removed in the free decay test. Hence, the more reliable damping parameter would be expected to be the second one.

4.2. MDOF CABLE STRUCTURE

First, the translational mode was investigated. Figure 8(a) shows a plot of restoring force versus displacement obtained from a forced vibration test with a single shaker applying a ramped sinusoid at 8·5 Hz to the centre of mass of the beam. Figure 8(b) shows a plot of restoring force, estimated from acceleration measurements during a free decay test.

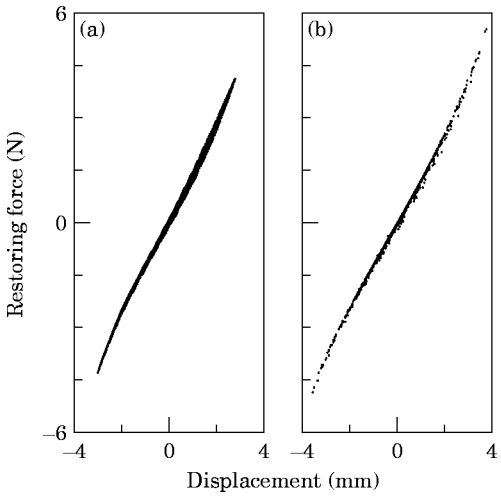

Figure 8. Restoring force plots for translational mode of MDOF system: (a) forced vibration; (b) free decay.

As for the SDOF experiment, the error e has been calculated as a function of the number of system parameters included in the model; see Figure 9, and the results are similar to those obtained previously. Again, it is found that the inclusion of stiffness terms up to the third order and of a single damping term leads to the error being reduced to 0·016. The initial error, if only linear stiffness and no damping are considered, is 0·08. As in the SDOF experiment, it is found that little improvement is achieved by considering further terms, the lowest error being 0·012 when the maximum number of terms are considered. Hence, it is concluded that a reasonable fit to the experimental data can be obtained by including the terms m_1, c_{11}, k_{11}, and k_{13} in the system model and the values that are estimated from the two sets of experimental data are given in Table 2. Note that, as in the SDOF experiment, the free decay experiment is unable to estimate the mass of the system because the external force is zero.

To investigate the rotation mode an initial test was carried out with a single shaker placed at one end of the Al-alloy beam. However, because of the high rotational stiffness of the two-cable system, only small amplitude rotations were excited and the response was found to be mainly linear, thus giving poor quality estimation of the non-linear stiffness terms of the system.

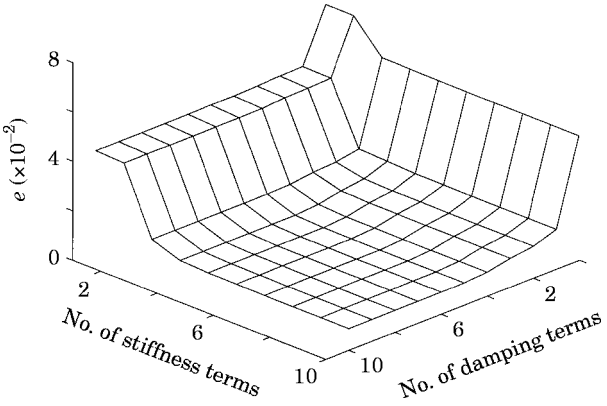

Figure 9. Error plot for MDOF system (translational mode, shaker test).

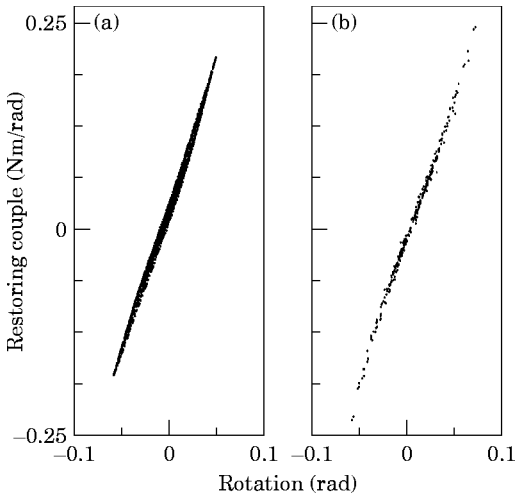

Figure 10. Restoring couple plots for rotation mode of MDOF system: (a) forced vibration; (b) free decay.

Therefore, a further set of tests were conducted with two shakers applying excitation in anti-phase. By varying the excitation amplitude of each shaker separately, suitable rotation levels were achieved. Free decay tests were also carried out, the system being released after imposing both a translation and a rotation to the block.

Figure 10 shows plots of the restoring couple obtained from these two tests. Note that, in analogy with the free decay test of the translation mode, the value of the moment of inertia of the block has to be known before calculating the values of the restoring couple.

Because of the coupling between rotation and translation modes, the error e depends on three different types of terms, which makes it impossible to show graphically the variation of e as the number of each type of terms is varied. Figure 11 shows the variation of e with the number of direct stiffness terms, i.e., the terms k_{2j} in equation (3), and with the number of damping terms c_{2j}. The number of coupled stiffness terms is set at 1.

As in the previous cases, the error e bottoms out once the physically meaningful terms have been included. Note that the effect of including a quadratic stiffness term again has a negligible effect on reducing the error. This error plot shows that there is little point in including terms other than m_2, c_{21}, k_{21}, k_{23} (and k_{1221}) in the model of the rotation mode.

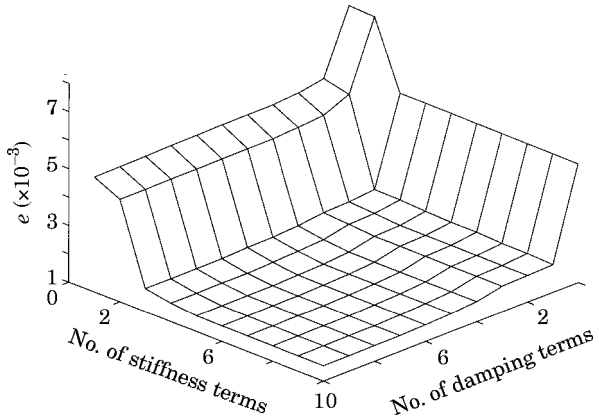

Figure 11. Error plot for MDOF system (rotation mode, shaker test).

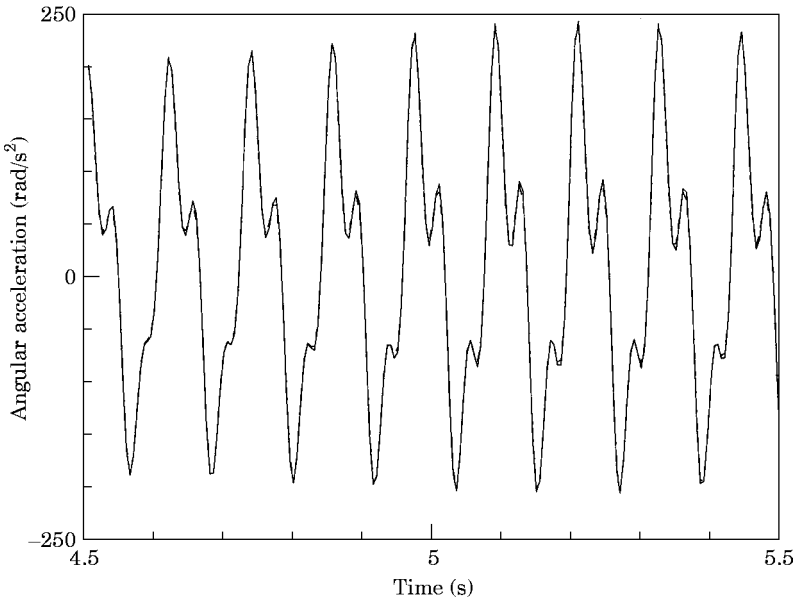

Figure 12. Comparison between measured (——) and estimated (– – –) acceleration responses.

Hence, the values of these parameters have been estimated by the identification algorithm and are given in Table 2.

As a final check on the quality of the estimated parameters, a fourth order Runge–Kutta integration of the equations of motion was carried out, using the estimated system parameters, and the measured shaker force as input. The acceleration response estimated from this procedure practically coincides with the measured acceleration; see Figure 12.

5. DISCUSSION AND CONCLUSIONS

The main results that have emerged from this study are as follows. First, the particular implementation of the restoring force method presented in this paper, based on the singular value decomposition of the experimental data matrix **A**, is accurate and reliable. Second, the identification procedure should aim for only a small number of key system parameters, whose inclusion in the equations of motion yields substantial reductions in the mis-match between the measured response of the system and its analytical model. It is pointless to pursue the absolute minimum of the error function, which is sensitive to noise in the data. Third, it must be ensured that the experimental data covers a sufficient range to include all expected non-linearities, in order to fully represent the restoring force map. Fourth, shaker test data tends to produce more accurate estimates of non-linear stiffness parameters but overestimates damping. Better estimates of the damping coefficients are obtained from free decay tests. It is believed that these results will apply to other lightweight systems, with larger numbers of degrees of freedom.

The next stage in this study will be the application of the identification procedure established in this paper to the cable-stiffened deployable structures that have been recently developed by our group. These structures [11] exhibit non-linear dynamic behaviour, but the main source of non-linearity appears to be energy dissipation at the joints.

ACKNOWLEDGMENTS

Financial support from the Ministry of Defence, Singapore, in the form of a Defence Technology Training Award for G. E. B. Tan is gratefully acknowledged.

REFERENCES

1. K. Worden and G. R. Tomlinson 1991 *Proceedings of the 9th International Modal Analysis Conference*, 757–764. An experimental study of a number of nonlinear sdof systems using the restoring force surface method.
2. E. F. Crawley and A. C. Aubert 1986 *American Institute of Aeronautics and Astronautics Journal* **24**, 155–162. Identification of nonlinear structural elements by force-state mapping.
3. M. A. Al-Hadid and J. R. Wright 1990 *Mechanical Systems and Signal Processing* **4**, 463–482. Application of the force-state mapping approach to the identification of non-linear systems.
4. K. Worden, J. R. Wright, M. A. Al-Hadid and K. S. Mohammed 1994 *International Journal of Analytical and Experimental Modal Analysis* **9**, 35–55. Experimental identification of multi degree of freedom nonlinear systems using restoring force methods.
5. B. P. Masters and E. F. Crawley 1994 *American Institute of Aeronautics and Astronautics Journal* **32**, 2276–2285. Multiple degree-of-freedom force state component identification.
6. S. Pellegrino 1990 *International Journal of Solids and Structures* **26**, 1329–1350. Analysis of prestressed mechanisms.
7. S. Pellegrino 1992 *International Journal of Space Structures* **7**, 127–142. A class of tensegrity domes.
8. K. Worden 1990 *Mechanical Systems and Signal Processing* **4**, 295–319. Data processing and experiment design for the restoring force surface method. Part I: Integration and differentiation of measured time data.
9. G. Golub and C. Van Loan 1983 *Matrix computations*. North Oxford: Academic Press.
10. S. Pellegrino 1986 *Ph.D. Thesis*, *University of Cambridge*. Mechanics of kinematically indeterminate structures.
11. A. S. K. Kwan, Z. You and S. Pellegrino 1993 *International Journal of Space Structures* **8**, 29–40. Active and passive cable elements in deployable/retractable masts.